



ESA Climate Change Initiative
cloud_cci

Algorithm Theoretical Basis Document (ATBD)
of the Community Code for Climate (CC4CL)
Multi Layer Cloud (CC4CL-MLEV) module

Version 1.1

Caroline A. Poulsen¹, Gareth E. Thomas¹, Richard Siddans¹, Greg McGarragh², Elisa Carboni²

¹Space Science and Technology Department, Rutherford Appleton Laboratory, Chilton, Didcot, OX11 0QX,
UK

²Atmospheric, Oceanic and Planetary Physics, University of Oxford, Oxford, OX1 3PU, UK



Contents

1	Introduction	3
2	Algorithm description	3
2.1	Cloud property retrieval algorithm	4
2.1.1	Cloud / Atmosphere / Surface Model	5
2.1.2	Reflectance and transmission operators	6
2.1.3	Surface reflectance operators	7
2.1.4	Single layer Visible and near-IR RTM	8
2.1.5	Single layer Thermal-IR RTM	10
2.1.6	Single layer Measurement vector and covariance	11
2.1.7	ECMWF data	11
2.1.8	Quality Control	12
2.1.9	Derivatives of the forward model	12
2.2	Extension to a fast 2-layer cloud forward model	12
2.2.1	2 layer SOLAR fast FM - VIS	12
2.3	Thermal brightness temperature (2 layers)	13
2.3.1	Multi layer measurement and state vector, a priori and covariance information	15
3	Input and output data	16



Date	Change	Person
03/03/2016	Original Version	Caroline Poulsen
23/05/2016	Updates after Review by S. Pinnock	Caroline Poulsen

1 Introduction

A widely recognised shortcoming of visible-infrared cloud retrievals is the common assumption of a single cloud layer. Mace et al. (2009) showed that multi-level clouds account for approximately 60% of all cloudy scenes; assuming a single layer model in these situations will result in biases in retrieved cloud properties. Different retrieval techniques, relying on the different radiative features of different instrument channels, will show differing bias due to this approximation. In the case of optically thick high-level clouds, these biases will be relatively minor, for example the cloud top height/pressure and temperature, and the effective radius, for which the retrieval has its peak sensitivity at approximately one optical depth into the cloud, will be close to the true values of the upper layer. The retrieved optical depth will be representative of the total cloud column however. Multi-layer cloud retrieval biases will be at their strongest in the frequently encountered Heidinger et al. [2005] case of optically thin high level cirrus overlaying lower level cloud. For retrievals which rely on channels in the thermal infrared (especially window channels) for their sensitivity to cloud height, such as the long-term heritage channel ECV product to be produced in the baseline Cloud CCI project, the radiance observed will be a combination of emission from both upper and lower clouds. This results in retrieved height/pressure/temperature which lies somewhere between the two clouds, and the retrieved effective radius is affected in a similar way Poulsen et al. [2012]. Although it is often not possible to accurately fit the observed spectral radiance of thin cirrus over low-level cloud with a single layer model, resulting in an elevated retrieval cost function and large uncertainties in the state parameters in an optimal estimation retrieval scheme (such as CC4CL), this is not always a reliable method of detecting multi-level clouds. Comparisons with active sensors, such as CALIPSO and CloudSat, show that in some cases a multi-level cloud does provide a good radiance fit. Conversely, there are many other situations which can result in a poor retrieval fit.

This document describes an optimal estimation retrieval scheme for the derivation of the multiple layers of cloud properties from top-of-atmosphere (TOA) radiances measured by satellite-borne visible-IR radiometers. The algorithm is based on the single layer retrieval of clouds as described in greater detail by Poulsen et al. [2012], McGarragh et al. [2016] and Watts et al. [1998]. The algorithm makes up part of the Community Code for CLimate (CC4CL) retrieval scheme (the other part, known as ORAC, performs aerosol retrievals and is described in Thomas et al. [2010]).

Specific features of this algorithm include:

- A full implementation of the optimal estimation framework described by Rodgers [2000], enabling rigorous error propagation and inclusion of *a priori* knowledge.
- A common retrieval algorithm over both land and ocean, with only the *a priori* constraint on the surface reflectance differing between the two.
- Consistent and simultaneous retrieval of all cloud parameters in both layers in the visible and infrared.

2 Algorithm description

The following sections provide a detailed description of the CC4CL Multi layer algorithm. In the first sections the single layer model is described while in section 2.2 the extension of the single layer model to retrieve multi layer clouds in the thermal and solar domains is described.



2.1 Cloud property retrieval algorithm

The algorithm described here is applicable to measurements from instruments with a sufficient set of visible to thermal infrared atmospheric window channels. The baseline CC4CL retrieval is applied to 5 heritage channels in order to produce a long consistent time series of cloud properties, the multi layer model retrieves more information on the vertical structure and hence requires additional information from extra channels than those used in the CC4CL heritage product. The multi layer cloud retrieval has been developed using the MODIS instrument and the .67, .87, 1.6, 3.7, 7.3, 8.7, 11,12, 13 μ m channels. These channels are sensitive in different ways to the macro and microphysical properties of cloud. For example, the infrared channels compliment the visible channels in the case of optically thin clouds. It is necessary to include a channel sensitive to water vapour or vertical structure of the cloud such as the 8.7 μ m channel or an O2-Aband channel in order to retrieve information on 2 layers. However it should be noted that in the combined visible/IR retrieval described here the observations are not sensitive to every aspect of the three-dimensional distribution of all relevant cloud properties and no single channel is uniquely sensitive to a specific cloud property.

We approach the problem of extracting useful information on cloud as an inverse problem. A forward model (FM) is defined which applies a radiative transfer model (RTM) to simulate satellite radiances based on a parametrised cloud / atmosphere / surface model (CM) and the prescribed observing conditions. An inverse or retrieval model (RM) is then used to obtain the cloud parameters which give the best fit between the model predicted and observed radiances, taking into account measurement uncertainties and relevant prior knowledge. This inverse problem is solved using the optimal estimation method [Rodgers, 2000] (OEM).

The basic principle of the OEM is to maximise the probability of the retrieved state, conditional on the value of the measurements and any *a priori* knowledge. Formally, it maximises the conditional probability $P = P(\vec{x}|\vec{y}, \vec{x}_a)$ with respect to the values of the measurement vector \vec{y} , state vector \vec{x} , and *a priori* estimate of the state \vec{x}_a (i.e. the most likely state prior to considering the measurements). It is assumed that errors in the measurements, forward model and *a priori* parameters are normally distributed with zero mean and covariances given by \mathbf{S}_y and \mathbf{S}_a , respectively. The solution state is found by minimising the cost function J :

$$J(\vec{x}) = [\vec{y}(\vec{x}) - \vec{y}_m] \mathbf{S}_y^{-1} [\vec{y}(\vec{x}) - \vec{y}_m]^T + (\vec{x} - \vec{x}_a) \mathbf{S}_a^{-1} (\vec{x} - \vec{x}_a)^T. \quad (1)$$

Starting from some initial guess of the state and linearising the forward model, the gradient of the cost function is estimated. Using that, a state is selected which is predicted to have lower cost. The Levenberg-Marquart [Marquardt, 1963, Levenberg, 1944] scheme is used to perform the minimisation. The procedure is iterated until the change in cost between iterations is less than $0.05m$, where m is the length of \vec{y} , (called convergence) or the retrieval is abandoned after 25 iterations.

If the *a priori* and measurement uncertainties are well represented by their respective covariances, the value of the cost function at solution is expected to be sampled from a χ^2 distribution with degrees of freedom (approximately) equal to the total number of elements in the measurement and state vectors. Hence, J at convergence provides a measure of the likelihood of the solution-state being consistent with observations and prior knowledge.

For retrievals which satisfactorily converge, i.e. converge to a minimum cost which is consistent with measurement and prior uncertainties, the uncertainty on the estimated state parameters is described by the solution covariance

$$\mathbf{S}_x = (\mathbf{K}^T \mathbf{S}_y^{-1} \mathbf{K} + \mathbf{S}_a^{-1})^{-1}, \quad (2)$$

where \mathbf{K} contains the derivatives of the forward model with respect to each solution state parameter:

$$K_{i,j} = \frac{\partial y_i}{\partial x_j}. \quad (3)$$



2.1.1 Cloud / Atmosphere / Surface Model

The single layer retrieval forward model can be considered to consist of three components: a scattering cloud layer is located within a clear-sky atmosphere over a surface of known reflectance/emissivity. The clear-sky atmosphere is defined by temperature and humidity profiles taken from ECMWF ERA Interim analyses [Dee et al., 2008]. As only window channels are being used in the retrieval, the influence of variations in trace gas concentrations, as well as the uncertainties in ECMWF water vapour profiles, are well within the measurement noise.

The surface is characterised by a bidirectional reflectance distribution function (BRDF) which is computed differently for ocean and land surface. The BRDF over ocean is computed using the methodology outlined by [Sayer et al., 2010] which includes 3 components:

$$\rho(\theta_0, \theta_v, \phi, \lambda, u, v) = \rho_{sg}(\theta_0, \theta_v, \phi, \lambda, u, v) + \rho_{wc}(\lambda, u, v) + \rho_{ul}(\theta_0, \theta_v, \lambda, C), \quad (4)$$

where ρ_{sg} is the sun-glint off wave facets [Cox and Munk, 1954a], ρ_{wc} is the reflectance from surface foam, so-called “whitecaps” [Koepeke et al., 1984], and ρ_{ul} is the scattering from the within the water, so-called “underlight” [Morel et al., 1977]. In addition, physical parameters include the horizontal wind vector u and v (m/s) and the ocean pigment concentration C (mg/m^3).

The BRDF over land is a weighted sum of an isotropic kernel (unity) and two BRDF kernels [Wanner et al., 1997]

$$\rho(\theta_0, \theta_v, \phi, \lambda) = f_{iso}(\lambda) + f_{vol}(\lambda)K_{vol}(\theta_0, \theta_v, \phi) + f_{geo}(\lambda)K_{geo}(\theta_0, \theta_v, \phi), \quad (5)$$

where $K_{vol}(\theta_0, \theta_v, \phi)$ is known as the the Ross-thick kernel which parameterises *volumetric* scattering of leaves in dense vegetation and $K_{geo}(\theta_0, \theta_v, \phi)$ is the Li-sparse kernel which parameterises *geometric* shadowing in sparsely wooded vegetation. The weights $f(\lambda)$ are provided by the 0.05° MODIS MCD43C1 BRDF auxiliary input discussed in section 3.

For the infrared channels the surface is assumed to have an emissivity of unity over the ocean, while the CIMSS global land emissivity database is used [Seemann et al., 2007]. The temperature of the surface is a retrieved parameter.

Each measurement pixel is considered to be either fully cloudy or clear. The algorithm does provide the capability of retrieving the cloud-filled fraction of a pixel, but it has been found that the heritage channels do not provide sufficient information to distinguish thin but complete cloud cover from thick but partial cover. Cloud is assumed to be a single, plane-parallel layer of either liquid or ice particles. The layer is assumed to be (geometrically) infinitely thin and is placed within the clear-sky atmosphere model. The cloud layer is parametrised in terms of the following retrieved quantities:

- The cloud phase, i.e. ice or liquid.
- The effective radius r_{eff} of the cloud particle size distribution.
- The total (vertically integrated) optical depth τ of the cloud at a fixed wavelength of $0.55 \mu\text{m}$.
- The cloud top pressure p_c .

Size distributions for ice and liquid cloud are defined as a function of only r_{eff} , which defines the shape of the modelled size distribution, and τ , implicitly defining the total number of particles. For ice clouds, single-scattering properties (extinction coefficient, single-scattering albedo and phase function) are taken from Baran et al. [2004]. These are based on a mixture of ray tracing and T-Matrix methods. Size distributions are those of warm Uncinus cirrus cloud [Takano et al., 1989] which have been scaled to give a range of effective



radii. Single-scattering properties of liquid cloud are derived by Mie theory assuming a modified gamma size distribution of particle radius r such that

$$n(r) = 2.373 r^6 \exp\left(\frac{-6r}{r_m}\right), \quad (6)$$

where r_m is the mode radius of the distribution. The radiatively significant effective radius r_{eff} is given by

$$r_{\text{eff}} = \frac{\int_0^\infty r \pi r^3 n(r) dr}{\int_0^\infty \pi r^2 n(r) dr}. \quad (7)$$

This approach reduces the complexity of cloud to a simple model with parameters which can be distinguished using the heritage channels. The visible channel radiances are predominantly controlled by the cloud optical depth. Near-IR channels are also sensitive to particle size and phase due to the dependence on size of the single-scattering albedo in that spectral range and the associated differences between ice and liquid phase particles. Thermal channels predominantly provide information on cloud top pressure (via the dependence of the cloud thermal emission on the atmospheric temperature profile). It should be appreciated that all channels are sensitive, to a greater or lesser extent, to all parameters (dependent on the scene).

This simple model cannot represent all aspects of cloud three-dimensional structure. In the ideal case, the retrieved parameters should correspond to vertical (over the profile) and horizontal (over the scene) averages of the “true” cloudy properties. However, there are classes of clouds, particularly those with strong vertical variations in particle size and phase, for which this model cannot predict radiances consistent with observations in all channels. Such conditions can be identified by checking that the retrieval converges with satisfactory cost. This feature can be used to identify multi layer cloud scenarios for when application of multi layer cloud retrievals will improve results.

2.1.2 Reflectance and transmission operators

The next step in the forward model is the prediction of transmission and reflectance operators for an atmosphere *without* molecular absorption. This calculation is based on solar and viewing geometry, the molecular scattering optical thickness τ_{ms} and single-scattering phase function $P_{\text{ms}}(\lambda, \Theta)$, the optical thickness $\tau_a(\lambda)$, the single-scattering albedo $\omega_a(\lambda)$ and the single-scattering phase function $P_a(\lambda, \Theta)$. For performance reasons this calculation is look-up table (LUT) based from which the values for an arbitrary set of geometric and optical parameters may be interpolated. The vertices of the LUTs are computed with the DIScrete Ordinates Radiative Transfer (DISORT) software package [Stamnes et al., 1988]. It is important to note that this step, although slow, is performed off-line and the resulting look-up tables (LUTs) are static.

DISORT is a thoroughly documented and widely used general purpose algorithm for the calculation of time-independent radiative transfer. The DISORT algorithm solves the equation for the transfer of monochromatic light at wavelength λ in a medium with absorption and multiple scattering, including solar and thermal sources. The radiative transfer equation is written as

$$\mu \frac{dL_\lambda(\tau_\lambda, \mu, \phi)}{d\tau} = L_\lambda(\tau_\lambda, \mu, \phi) - J_\lambda(\tau_\lambda, \mu, \phi), \quad (8)$$

where $L_\lambda(\tau_\lambda, \mu, \phi)$ is the intensity along direction μ, ϕ (where μ is the cosine of the zenith angle and ϕ is the azimuth angle) at optical depth τ_λ measured perpendicular to the surface of the medium. $J_\lambda(\tau_\lambda, \mu, \phi)$ is the source function, which can include solar and thermal sources.

It should be noted that DISORT still makes some important approximations, which can limit its accuracy in certain circumstances. The most important of these are:

- It assumes a plane parallel atmosphere, which makes it inapplicable at viewing or zenith angles above approximately 75° , where the curvature of the Earth has a significant influence on radiative transfer.



- It is a one-dimensional model, so cannot reproduce the effects of horizontal gradients in the scattering medium. This is important where strong gradients exist, such as near cloud edges.
- It does not model polarisation effects and hence cannot be used to model measurements made by instruments which are sensitive to polarisation and does not take into account the polarisation introduced into the diffuse component of radiance by molecular scattering.

DISORT is provided with solar and instrument geometry, the molecular scattering and cloud radiative properties at the vertexes. The transmission and reflectance of the atmosphere is computed for both direct beam and diffuse radiation sources separately. The calculations are performed quasi-monochromatically, i.e. a single radiative transfer calculation is performed for each channel. It is the input optical properties that are convolved to the instrument's response function for a particular channel. These calculations produce six LUTs for each channel:

- $R_{bb}(\theta_0, \theta_v, \phi)$: the bidirectional reflectance of the cloud.
- $T_{bb}^\downarrow(\theta_0)$: the downward direct transmission of the cloud of the direct solar beam.
- $T_{bb}^\uparrow(\theta_v)$: the upward direct transmission of the cloud into the viewing direction.
- $T_{bd}^\downarrow(\theta_0)$: the downward diffuse transmission of the cloud, as illuminated by the direct solar beam.
- $T_{db}^\uparrow(\theta_v)$: the upward diffuse transmission of the cloud, as viewed from a specific direction.
- R_{dd} : the bi-hemispherical reflectance of the cloud.

Here, a \downarrow denotes transmission from the top to the bottom of the atmosphere, while \uparrow indicates the reverse. Dependence on the solar zenith, viewing zenith and relative azimuth angles are denoted by θ_0 , θ_v and ϕ respectively. The pairs of b and d subscripts denote the type of radiation each term operates on and produces; for example $T_{bd}^\downarrow(\lambda, \theta_0)$ operates on the direct beam (b) of solar radiation, and produces the diffuse radiation (d) that results at the bottom of the atmosphere. Each of these tables contains tabulated transmission or reflectance (depending on the table) values for each of the ten equally spaced solar and/or sensor zenith angles, eleven equally spaced relative azimuth angles ($R_{bb}(\lambda, \theta_0, \theta_v, \phi)$ only), eighteen $0.55 \mu\text{m}$ optical depths and twenty three effective radii.

2.1.3 Surface reflectance operators

The CC4CL forward model works on the assumption that the surface BRDF can be parametrised by four reflectance terms:

1. The bidirectional reflectance, $\rho_{bb}(\lambda, \theta_0, \theta_v, \phi)$. This is the reflectance of the surface to direct beam illumination at θ_0 , as viewed from a specific direction θ_v . It is the reflectance that would be observed by a satellite instrument in the absence of an atmosphere.
2. The directional-hemispheric reflectance $\rho_{bd}(\lambda, \theta_0)$. This is the fraction of incoming direct beam illumination at θ_0 that is reflected across all viewing angles. This is also referred to as the *black-sky albedo*.
3. The hemispheric-directional reflectance $\rho_{db}(\lambda, \theta_v)$. This is the reflectance of the surface to purely diffuse illumination, as viewed from a specific direction θ_v .
4. The bi-hemispheric reflectance $\rho_{dd}(\lambda)$. This is the reflectance of the surface to purely diffuse illumination, across all viewing directions. This is also referred to as the *white-sky albedo*.



The first term $\rho_{bb}(\theta_0, \theta_v, \phi)$ is computed directly from the BRDF. The three other terms are derived from the BRDF integrated over solar and/or viewing geometry written as

$$\begin{aligned}\rho_{bd}(\lambda, \theta_0) &= \frac{\int_0^{2\pi} \int_0^{\pi/2} \rho_{bb}(\lambda, \theta_0, \theta_v, \phi) \cos \theta_v \sin \theta_v d\theta_v d\phi}{\int_0^{2\pi} \int_0^{\pi/2} \cos \theta_v \sin \theta_v d\theta_v d\phi} \\ &= \frac{1}{\pi} \int_0^{2\pi} \int_0^{\pi/2} \rho_{bb}(\lambda, \theta_0, \theta_v, \phi) \cos \theta_v \sin \theta_v d\theta_v d\phi,\end{aligned}\quad (9)$$

$$\begin{aligned}\rho_{db}(\lambda, \theta_v) &= \frac{\int_0^{2\pi} \int_0^{\pi/2} \rho_{bb}(\lambda, \theta_0, \theta_v, \phi) \cos \theta_v \sin \theta_v d\theta_0 d\phi}{\int_0^{2\pi} \int_0^{\pi/2} \cos \theta_v \sin \theta_v d\theta_0 d\phi} \\ &= \frac{1}{\pi} \int_0^{2\pi} \int_0^{\pi/2} \rho_{bb}(\lambda, \theta_0, \theta_v, \phi) \cos \theta_v \sin \theta_v d\theta_0 d\phi,\end{aligned}\quad (10)$$

$$\begin{aligned}\rho_{dd}(\lambda) &= \frac{\int_0^{\pi/2} \rho_{bd}(\lambda, \theta_0) \cos \theta_0 \sin \theta_0 d\theta_0}{\int_0^{\pi/2} \cos \theta_0 \sin \theta_0 d\theta_0} \\ &= 2 \int_0^{\pi/2} \rho_{bd}(\lambda, \theta_0) \cos \theta_0 \sin \theta_0 d\theta_0.\end{aligned}\quad (11)$$

2.1.4 Single layer Visible and near-IR RTM

Each short wave channel measures the radiance in the instrument's field-of-view, defined by the solid angle Δ_{FOV} . Each channel also has a relative spectral response $\rho(\lambda)$ within a wavelength interval $[\lambda_1, \lambda_2]$ and has zero response outside this band. Under these conditions the radiance measured by the instrument is

$$L_{\lambda}^r(\omega_r) = \frac{\int_0^{\Delta_{FOV}} \int_{\lambda_1}^{\lambda_2} L_{\lambda}^r(\lambda, \omega) \rho(\lambda) d\lambda d\omega}{\int_0^{\Delta_{FOV}} d\omega},\quad (12)$$

where ω is used to represent the spherical coordinate zenith and azimuth angle pair (θ, ϕ) and the integral over solid angle has been abbreviated as

$$\int_0^{\Delta\omega} d\omega = \int_0^{2\pi} \int_0^{\Delta\theta} \sin \theta d\theta d\phi.\quad (13)$$

The 'Sun-normalised radiance' (or top-of-atmosphere reflectance) can then be formed by dividing the measured radiance $L_{\lambda}^r(\omega_r)$ by E_{λ}^0 , the irradiance the satellite would measure if viewing the Sun through a perfect diffuser i.e.

$$R(\bar{\lambda}, \omega_0, \omega_r) = \frac{\pi L_{\lambda}^r(\omega_r)}{\cos \theta_0 E_{\lambda}^0}.\quad (14)$$

The factor $\cos \theta_0$ accounts for the reduction in energy per unit area when the Sun's energy strikes the atmosphere-Earth system at an angle θ_0 to the local vertical.

In the limit of a very narrow band, the measured Sun normalised radiance is a good approximation to the spectral bidirectional reflectance factor $R(\lambda, \omega_i, \omega_r)$, which is defined as the ratio of the reflected radiant flux to the reflected radiant flux from an ideal diffuse (i.e. Lambertian) surface [Schaeppman-Strub et al., 2006]. The bidirectional reflectance factor is a function of the wavelength λ and the input and output directions

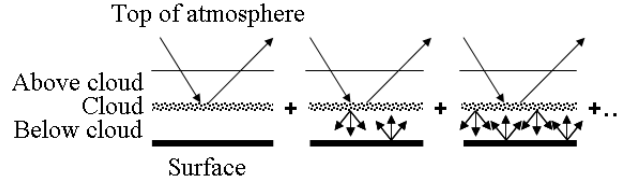


Figure 1: Schematic of the contributions to the measured radiance through multiple scattering between the atmosphere and surface.

(represented by ω_i and ω_r , respectively). For simplicity, the dependence of reflection and transmittance on λ will not be explicitly shown.

The cloudy fraction of the atmosphere in a scene is modelled with three layers: a below-cloud layer, a cloud layer and an above-cloud layer. The above and below-cloud layers consist of gaseous absorbers that attenuate radiation without scattering¹.

The gaseous absorption optical depth of the atmosphere is calculated using visible channel coefficients for RTTOV version 11.0 and the clear sky contribution for each scene is calculated with NWP information provided by 6-hourly ECMWF ERA Interim analyses. This total absorption optical depth is then partitioned into the above-cloud optical depth τ_{ac} and the below-cloud optical depth τ_{bc} based on the cloud top pressure relative to the surface pressure.

Using the reflectance and transmission operators described in section 2.1.2, the surface reflectance description in section 2.1.3, and by neglecting molecular absorption, the observed reflectance of the atmosphere/surface system can be written as (assuming dependence on wavelength λ):

$$\begin{aligned}
 R(\theta_0, \theta_v, \phi) = & R_{bb}(\theta_0, \theta_v, \phi) && \text{Reflection off the atmosphere} \\
 & + T_{bb}^\downarrow(\theta_0) \rho_{bb}(\theta_0, \theta_v, \phi) T_{bb}^\uparrow(\theta_v) \\
 & + T_{bb}^\downarrow(\theta_0) \rho_{bd}(\theta_0) T_{db}^\uparrow(\theta_v) \\
 & + T_{bd}^\downarrow(\theta_0) \rho_{db}(\theta_v) T_{bb}^\uparrow(\theta_v) \\
 & + T_{bd}^\downarrow(\theta_0) \rho_{dd} T_{db}^\uparrow(\theta_v) \\
 & + T_{bb}^\downarrow(\theta_0) \rho_{bd}(\theta_0) R_{dd} \rho_{db} T_{bb}^\uparrow(\theta_v) \\
 & + T_{bb}^\downarrow(\theta_0) \rho_{bd}(\theta_0) R_{dd} \rho_{dd} T_{db}^\uparrow(\theta_v) \\
 & + T_{bd}^\downarrow(\theta_0) \rho_{dd} R_{dd} \rho_{db} T_{bb}^\uparrow(\theta_v) \\
 & + T_{bd}^\downarrow(\theta_0) \rho_{dd} R_{dd} \rho_{dd} T_{db}^\uparrow(\theta_v) \\
 & + T_{bb}^\downarrow(\theta_0) \rho_{bd}(\theta_0) R_{dd} \rho_{dd} R_{dd} \rho_{db} T_{bb}^\uparrow(\theta_v) \\
 & + T_{bb}^\downarrow(\theta_0) \rho_{bd}(\theta_0) R_{dd} \rho_{dd} R_{dd} \rho_{dd} T_{db}^\uparrow(\theta_v) \\
 & + T_{bd}^\downarrow(\theta_0) \rho_{dd} R_{dd} \rho_{dd} R_{dd} \rho_{db} T_{bb}^\uparrow(\theta_v) \\
 & + T_{bd}^\downarrow(\theta_0) \rho_{dd} R_{dd} \rho_{dd} R_{dd} \rho_{dd} T_{db}^\uparrow(\theta_v) \\
 & + \dots
 \end{aligned}
 \tag{15}$$

Here we have four terms resulting from a single surface reflection in equation 15, which can be described as follows:

- $T_{bb}^\downarrow(\theta_0) \rho_{bb}(\theta_0, \theta_v, \phi) T_{bb}^\uparrow(\theta_v)$ is the direct transmission of the solar beam, reflected off the surface and transmitted directly to the satellite.
- In $T_{bb}^\downarrow(\theta_0) \rho_{bd}(\theta_0) T_{db}^\uparrow(\theta_v)$ the diffusely reflected portion of the directly transmitted solar beam is diffusely transmitted (via multiple scattering in the atmosphere) into the viewing direction of the satellite.

¹Molecular scattering throughout the atmospheric column is included in the scattering calculations carried out for the cloud layer



- $T_{bd}^{\downarrow}(\theta_0)\rho_{db}(\theta_v)T_{bb}^{\uparrow}(\theta_v)$ gives the portion of the diffusely transmitted solar beam, which is then reflected into the viewing direction of the satellite and directly transmitted back through the atmosphere.
- $T_{bd}^{\downarrow}(\theta_0)\rho_{dd}T_{db}^{\uparrow}(\theta_v)$ is the purely diffuse component, where solar radiation is diffusely transmitted to the surface, reflected off the surface and diffusely transmitted to the satellite.

The terms following on from these describe the rapidly diminishing series of multiple reflections between the surface and overlaying atmosphere. For these terms the assumption has been made that ground and atmosphere pair are essentially Lambertian reflectors (i.e. that only the bi-hemispherical reflectance of the atmosphere is needed). Neglecting directly transmitted solar radiation, this is equivalent to saying the sky is equally bright in all directions.

By gathering terms, equation 15 can be simplified to give

$$\begin{aligned}
 R &= R_{bb}(\theta_0, \theta_v, \phi) \\
 &+ T_{bb}^{\downarrow}(\theta_0)\rho_{bb}(\theta_0, \theta_v, \phi)T_{bb}^{\uparrow}(\theta_v) + T_{bd}^{\downarrow}(\theta_0)\rho_{db}(\theta_v)T_{bb}^{\uparrow}(\theta_v) \\
 &+ \left(T_{bb}^{\downarrow}(\theta_0)\rho_{bd}(\theta_0) + T_{bd}^{\downarrow}(\theta_0)\rho_{dd} \right) T_{db}^{\uparrow}(\theta_v) (1 + \rho_{dd}R_{dd} + \rho_{dd}^2R_{dd}^2 + \dots) \\
 &+ \left(T_{bb}^{\downarrow}(\theta_0)\rho_{bd}(\theta_0) + T_{bd}^{\downarrow}(\theta_0)\rho_{dd} \right) R_{dd}\rho_{db}(\theta_v)T_{bb}^{\uparrow}(\theta_v) (1 + \rho_{dd}R_{dd} + \rho_{dd}^2R_{dd}^2 + \dots).
 \end{aligned} \tag{16}$$

This can then be further simplified, using the appropriate series limit, to give

$$\begin{aligned}
 R &= R_{bb}(\theta_0, \theta_v, \phi) \\
 &+ T_{bb}^{\downarrow}(\theta_0)\rho_{bb}(\theta_0, \theta_v, \phi)T_{bb}^{\uparrow}(\theta_v) + T_{bd}^{\downarrow}(\theta_0)\rho_{db}(\theta_v)T_{bb}^{\uparrow}(\theta_v) \\
 &+ \frac{\left(T_{bb}^{\downarrow}(\theta_0)\rho_{bd}(\theta_0) + T_{bd}^{\downarrow}(\theta_0)\rho_{dd} \right) \left(T_{db}^{\uparrow}(\theta_v) + R_{dd}\rho_{db}(\theta_v)T_{bb}^{\uparrow}(\theta_v) \right)}{1 - \rho_{dd}R_{dd}}.
 \end{aligned} \tag{17}$$

Finally, the observed TOA reflectance including molecular absorption is obtained by scaling the terms in equation 17 by the appropriate clear-sky transmission terms

$$\begin{aligned}
 R_{TOA} &= \mathcal{T}_{ac}(\theta_0)\mathcal{T}_{ac}(\theta_v) [R_{bb}(\theta_0, \theta_v, \phi) \\
 &+ \mathcal{T}_{bc}(\theta_0)T_{bb}^{\downarrow}(\theta_0)\rho_{bb}(\theta_0, \theta_v, \phi)T_{bb}^{\uparrow}(\theta_v)\mathcal{T}_{bc}(\theta_v) + \mathcal{T}_{bc}(0)T_{bd}^{\downarrow}(\theta_0)\rho_{db}(\theta_v)T_{bb}^{\uparrow}(\theta_v)\mathcal{T}_{bc}(\theta_v) \\
 &+ \frac{\left(\mathcal{T}_{bc}(\theta_0)T_{bb}^{\downarrow}(\theta_0)\rho_{bd}(\theta_0) + \mathcal{T}_{bc}(0)T_{bd}^{\downarrow}(\theta_0)\rho_{dd} \right) \left(\mathcal{T}_{bc}(0)T_{db}^{\uparrow}(\theta_v) + R_{dd}\mathcal{T}_{bc}^2(0)\rho_{db}(\theta_v)T_{bb}^{\uparrow}(\theta_v)\mathcal{T}_{bc}(\theta_v) \right)}{1 - \rho_{dd}R_{dd}\mathcal{T}_{bc}^2(0)}] ,
 \end{aligned} \tag{18}$$

where $\mathcal{T}_{ac}(\theta) = e^{-\tau_{ac}/\cos\theta}$, $\mathcal{T}_{bc}(\theta) = e^{-\tau_{bc}/\cos\theta}$, τ_{ac} and τ_{bc} are the above cloud and below cloud optical thicknesses, respectively, and it is assumed that the mean angle of diffuse transmission is 66° .

2.1.5 Single layer Thermal-IR RTM

The thermal RTM makes extensive use of the RTTOV model [Saunders et al., 1999]. RTTOV directly provides the modelled radiance from the clear-sky fraction of the scene.

The observed cloudy brightness temperature is given by

$$L^{\uparrow}(\theta_v) = L_{ac}^{\uparrow}(\theta_v) + \left(L_{ac}^{\downarrow}R_{db}^{\uparrow}(\theta_v) + B(T_c)\varepsilon_c + L_{bc}^{\uparrow}T_{db}^{\uparrow}(\theta_v) \right) e^{-(\tau_{ac}/\cos\theta_v)}, \tag{19}$$

where $L_{ac}^{\uparrow}(\theta_v)$ is the upward radiance into the viewing direction from the atmosphere above the cloud, L_{ac}^{\downarrow} is the downward radiance from the atmosphere above the cloud, L_{bc}^{\uparrow} is the upward radiance from the atmosphere below the cloud, $B(T_c)$ is the Planck function as a function of the cloud top temperature T_c , ε_c is the



cloud emissivity obtained from an LUT computed in a similar way as those for the operators R and T and $e^{-(\tau_{ac}/\cos\theta_v)}$ is the transmission from TOA to the cloud top. The transmission term $e^{-(\tau_{ac}/\cos\theta_v)}$ is obtained from transmission profiles computed with RTTOV while the clear-sky radiance terms L are obtained from thermal emission profiles computed with RTTOV.

2.1.6 Single layer Measurement vector and covariance

The retrieval scheme described here uses nadir-view observations in the 0.67, 0.87, 1.6, 3.7, 11 and 12 μm channels. In practice only one of the 1.6 or 3.7 μm channels is included in a given retrieval because it has been found to be difficult to consistently represent both the 1.6 and 3.7 μm channels with the simple CM used [Baran et al., 2004]. Similarly, forward view radiances are not included as the three-dimensional structure of cloud will often cause differences between the views which cannot be accommodated by the simple model. The error covariance used in the retrieval is the sum of three terms:

$$\mathbf{S}_y = \mathbf{S}_{\text{noise}} + \mathbf{S}_{\text{pixel}} + \mathbf{S}_{\text{fm}}. \quad (20)$$

- $\mathbf{S}_{\text{noise}}$ represents random instrument noise on the observations. The matrix is assumed diagonal with values on the diagonal equal to the square of the assumed measurement noise, which are set for each instrument based on pre-launch characterisation.
- $\mathbf{S}_{\text{pixel}}$ represents errors related to inadequacies of the plane-parallel cloud model and imperfect co-registration of the channels. It is assumed diagonal and equal to the square of 2% of the measured radiance for visible and near-IR channels², and 0.08 K for the thermal channels. These are combined for the mixed 3.7 μm channel³. See Watts et al. [1998] for the derivation of this term.
- \mathbf{S}_{fm} is zero for rows and columns corresponding to thermal channels. For the visible and near-IR channels, the matrix represents uncertainties in the MODIS surface albedo. Diagonal elements are set to (the square of) 20% of the albedo for the corresponding channel. Off-diagonals are set to give a correlation between the visible/near-IR channels of 0.2.

2.1.7 ECMWF data

Clear-sky atmospheric radiances and transmittances are determined by RTTOV. This requires meteorological information as an input, which is provided by ECMWF ERA Interim reanalysis fields [Dee et al., 2008]. The required data⁴ are stored in one or more files of NetCDF or GRIB format. The data presents values and profiles representative of the atmosphere and surface at each point on a reduced Gaussian grid (with resolution dependent on the data source). ORAC retrieves states averaged over each satellite pixel and, to reduce computational expense, only evaluates RTTOV on a regular 500-by-500 latitude-longitude grid, which is then linearly interpolated onto each satellite pixel. (The errors from this process have been found to be less than the uncertainties in the RTTOV calculations themselves and so are considered negligible.)

The ECMWF data must be interpolated onto the ORAC grid. As the ECMWF data is generally on a coarser grid than that used by ORAC, the grid-cell average is approximated by the ECMWF value at the cell centre. The interpolation is performed using the EMOSLIB library provided by ECMWF (found at software.ecmwf.int/wiki/display/EMOS/Emoslib).

²For ATSR-2 channel 4, the visible uncertainty is 1.5%.

³For mixed channels, the radiance is converted into an equivalent brightness temperature.

⁴Currently, the fields `temperature`, `spec_hum`, `ozone`, `geopot`, `lnsp`, `sea_ice_cover`, `snow_albedo`, `sst`, `totcolwv`, `snow_depth`, `u10`, `v10`, `temp2`, `land_sea_mask` and `skin_temp` are required.



2.1.8 Quality Control

The quality of the CC4CL algorithm is based on the output diagnostics of the OE retrieval.

- The number of iterations: Indicates if the retrieval has converged.
- A convergence test: CC4CL uses the change in the cost function between iterations to determine whether a retrieval has converged.
- Cost function: If the cost function is approximately equal to the number of measurements then the retrieval is thought to have fit the model well. In practice, any retrieval with cost greater than ten times the number of measurements is considered suspect.
- Error estimates: If the previous criteria is satisfied then the uncertainty on the retrieved parameters is given in the solution covariance.

2.1.9 Derivatives of the forward model

The gradient of the forward model $\partial y_i / \partial x(j)$, where y_i is a radiance measurement in a single channel and x_j is one of the retrieved parameters, is required for the following purposes:

1. The gradient with respect to parameters which are to be derived from the measurements (state parameters) is a vital quantity for the inversion of the non-linear reflectance model by the Levenberg-Marquardt algorithm.
2. The gradient with respect to parameters which might be considered known and not part of the inversion procedure (model parameters such as surface reflectance spectral shape) is used to judge the sensitivity to these parameters and thus to estimate their contribution to the retrieval uncertainty.

Derivatives of the forward model may be obtained through straightforward linearisation of the forward model equations already given and as a result will not be listed here.

2.2 Extension to a fast 2-layer cloud forward model

This section describes the theoretical basis for a fast two-layer cloud forward model, suitable for use in retrievals. It should be noted that this model will have minimal effect on the heritage channel retrieval as a 2 layer model requires more information than the 'heritage' channels can provide. The model is applicable to instruments with any combinations of visible to infrared channels. It is currently demonstrated using SEVIRI and MODIS.

The model has been developed by extending the existing CC4CL LUT approach to deal with two layers. This is accomplished without modification to the contents of the RT LUTs themselves, only making use of existing variables to simulate interactions between both layers.

The visible 2 layer model is based the single layer model described in this ATBD. This model is effectively nested within itself, so that one call to the model computes the effective (surface + lower cloud) BRDF parameters which are fed into a second call to to represent the interaction with the upper cloud. The IR model explicitly models both layers in a separate, fast model.

2.2.1 2 layer SOLAR fast FM - VIS

To model a 2 layer cloud we consider the outgoing reflectance of the combined surface and lower-level cloud as a bidirectional reflectance underlying the upper layer. We consider the bidirectional reflectance applicable to the upper layer to be R for the lower layer, and the white and black sky albedo as following:



As illustrated in Fig.(3)

$$\begin{aligned}
 R_{black} &= R_{bd}(\theta_0) + T_{bb}^\downarrow(\theta_0)\rho_{bb}(\theta_0, \theta_v, \phi)T_{bd}^\uparrow(\theta_v) \\
 &+ T_{bb}\rho_{bd}(\theta_0)T_{dd} + T_{bd}^\downarrow(\theta_0)\rho_{dd}T_{dd} \\
 &+ T_{bb}\rho_{bd}(\theta_0)R_{dd}\rho_{dd}T_{dd} + T_{bd}^\downarrow(\theta_0)\rho_{dd}R_{dd}\rho_{dd}T_{dd} \\
 &+ \dots \\
 R_{black} &= R_{bd}(\theta_0) + T_{bb}^\downarrow(\theta_0)\rho_{bb}(\theta_0, \theta_v, \phi)T_{bd}^\uparrow(\theta_v) \\
 &+ (T_{bb}\rho_{bd}(\theta_0)T_{dd} + T_{bd}^\downarrow(\theta_0)\rho_{dd}T_{dd})(1 + R_{dd}\rho_{dd} + R_{dd}^2\rho_{dd}^2 + \dots) \\
 R_{black} &= R_{bd}(\theta_0) + T_{bb}^\downarrow(\theta_0)\rho_{bb}(\theta_0, \theta_v, \phi)T_{bd}^\uparrow(\theta_v) + \frac{(T_{bb}\rho_{bd}(\theta_0) + T_{bd}^\downarrow(\theta_0)\rho_{dd})T_{dd}}{(1 + R_{dd}\rho_{dd})} \quad (21)
 \end{aligned}$$

As in Fig.(4)

$$\begin{aligned}
 R_{white} &= R_{dd} + T_{dd}\rho_{dd}T_{dd} + T_{dd}\rho_{dd}R_{dd}\rho_{dd}T_{dd} + \\
 &+ T_{dd}\rho_{dd}R_{dd}^2\rho_{dd}T_{dd} + \\
 R_{white} &= R_{dd} + T_{dd}^2\rho_{dd}(1 + R_{dd}\rho_{dd} + R_{dd}^2\rho_{dd}^2 + \dots) \\
 R_{white} &= R_{dd} + \frac{T_{dd}^2\rho_{dd}}{1 - R_{dd}\rho_{dd}} \quad (22)
 \end{aligned}$$

Note: R_{black} , R_{white} and derivatives in the code are not black sky and white sky albedo but the equivalent term for sun normalised reflectance. This means for example that $R_{black}(code) = R_{black}(skyalbedo) \cos(\theta_0)$. The cloud parameters precomputed in the LUTs are all reflectances and transmittances except R_{bd} , this is not the cloud (or atmosphere for aerosol LUT) bidirectional reflectance but the equivalent value multiplied by $\cos(\theta_0)$. These sun normalised radiance computations are (in the code) obtained by multiplying the surface reflectance terms by $\cos(\theta_0)$ before passing them to the FM.

2.3 Thermal brightness temperature (2 layers)

We use a different notation for a two cloud layer model, as illustrated in the first part of Fig.(5). The atmospheric contributions are divided into: above, middle and below and indicated by the suffix 'a', 'm', 'b' respectively. The cloud parameters corresponding to higher cloud are indicated with '2', and the ones corresponding to the lower cloud are indicated with '1'.

The radiance reaching the satellite is considered the sum of the radiance going upward (L_1), the radiance reflected from the lower cloud layer (L_2) and the radiance reflected from the higher cloud layer (L_3). In this approximation we are neglecting the radiance reflected from the surface and the multiple reflections.

$$\mathcal{T}(\theta_v) = \frac{\mathcal{T}_{ac,2}(\theta_v)}{\mathcal{T}_{ac,1}(\theta_v)} \quad (23)$$

$$L^\uparrow(\theta_v) = \frac{L_{ac,2}^\uparrow - L_{ac,1}^\uparrow}{\mathcal{T}_{ac,1}(\theta_v)} \quad (24)$$

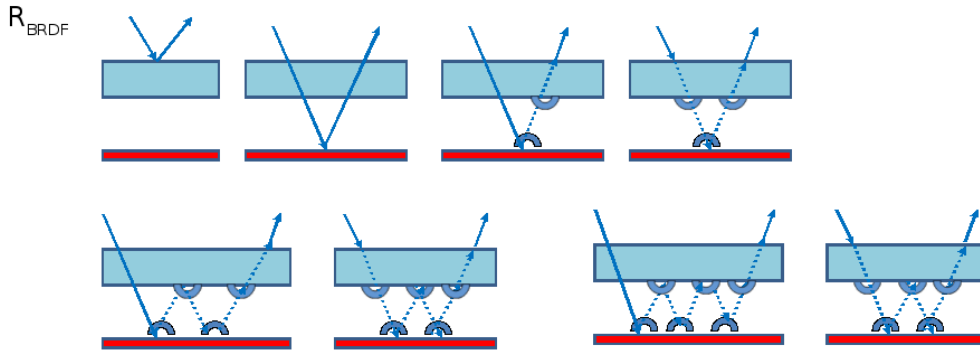


Figure 2: Scheme of the bidirectional reflectance for the surface-cloud layer system. The beam components are illustrated with arrows and continuous lines, the diffuse components with dotted lines and semicircles. This figure represents the first three orders of scattering between surface and cloud, the forward model takes into account all of them.

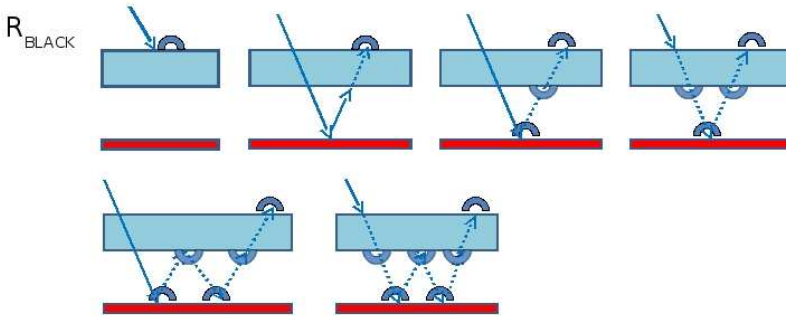


Figure 3: Scheme of the black sky albedo for the surface-cloud layer system.

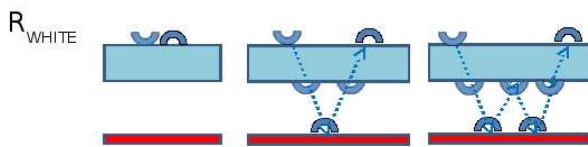


Figure 4: Scheme of the white sky albedo for the surface-cloud layer system.

$$L^\downarrow = L_{ac,2}^\downarrow - L_{ac,1}^\downarrow \mathcal{T}(\theta_v) \quad (25)$$

$$L_{over} = L_1 + L_2 + L_3 \quad (26)$$

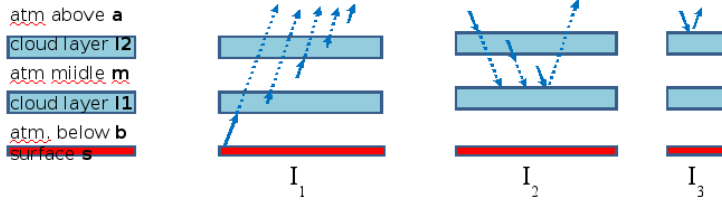


Figure 5: The first plot represents the IR notation for the 2 layer cloud model. The atmospheric contributions are divided into: above, middle and below and indicated with the suffix 'a', 'm', 'b' respectively. The cloud parameters corresponding to the higher cloud are indicated with '2', and the one corresponding to the lower cloud are indicated with '1'. L_1, L_2, L_3 are respectively the radiance going upward, the radiance reflected from the lower cloud layer and the radiance reflected from the higher cloud layer.

$$\begin{aligned}
 L_1 = & L_{bc,2}^\uparrow T_{db,2}^\uparrow(\theta_v) \mathcal{T}(\theta_v) T_{db,1}^\uparrow(\theta_v) \mathcal{T}_{ac,1}(\theta_v) \\
 & + B(T_C)_2 \epsilon_2 \mathcal{T}(\theta_v) T_{db,1}^\uparrow(\theta_v) \mathcal{T}_{ac,1}(\theta_v) \\
 & + B(T_C)_1 \epsilon_1 \mathcal{T}_{ac,1}(\theta_v) \\
 & + L_{db,1}^\uparrow T_{ac,1}^\uparrow(\theta_v) \mathcal{T}_{ac,1}(\theta_v) \\
 & + L_{ac,1}^\uparrow
 \end{aligned} \tag{27}$$

$$L_2 = \mathcal{T}(\theta_v) T_{db,1}^\uparrow(\theta_v) \mathcal{T}_{ac,1}(\theta_v) R_{bd,2}^\uparrow (L^\downarrow + B(T_C)_1 \epsilon_1 \mathcal{T}(\theta_v) + L_{ac,1}^\downarrow T_{db,1}^\uparrow(\theta_v) \mathcal{T}(\theta_v)) \tag{28}$$

$$L_3 = L_{ac,1}^\downarrow R_{bd,1}^\uparrow \mathcal{T}_{ac,1}(\theta_v) \tag{29}$$

2.3.1 Multi layer measurement and state vector, a priori and covariance information

Several retrieval experiments have been performed making use of different channel combinations, to test the ability of the 2 layer scheme to fit observations satisfactorily under the range of conditions encountered along an orbit.

Based on earlier non-linear tests Siddans et al. [2002] and experimental real retrievals, the following scheme has been implemented to carry out two-layer retrievals on real satellite data. The retrieval scheme described here uses nadir-view observations in the 0.67, 0.87, 1.6, 3.7, 8.7, 11 12 and 13 μm channels. Hence the retrieval is only applicable to satellites like MODIS and SEVIRI. While in the single layer model only one of the 1.6 or 3.7 μm channels is included in a given retrieval for the multi layer cloud using both channels may provide more information as ice is more absorbing in the 3.7 channel so the upper layer can dominate the signal at lower optical depths.

The state-vector used in the retrieval prescribes:

- Log_{10} optical depth, upper and lower layer;
- Cloud effective radius, upper and lower layer;
- Cloud top pressure, upper and lower layer;
- Surface temperature.



- Standard single-layer retrievals are performed. Under multi-layer conditions where the upper cloud is optically thin, these result in underestimated cloud-top heights and poor cost-function values at solution.
- Two-layer (ice over liquid) retrievals are performed for pixels where the single-layer scheme resulted in a high cost (>2 , for cost normalised by number of active channels). These are constrained by an estimated upper-layer CTH, estimated using a climatology of cloud top heights from Calipso.

An alternative technique to estimate the upper cloud top height is to assume that the height of ice cloud is correlated over relatively large scales in which case

- All retrievals within 30 image lines and columns of a given pixel are identified.
- Of these pixels, the ones for which the retrieved COT is larger than either 1 or the median COT in the region (if that is smaller than 1), are selected (to avoid, where possible, thin cloud with poorly estimated CTH).
- Of this subset of pixels, the 90th percentile value is taken as the *a priori* upper layer CTH (to avoid outliers which would be identified using the maximum value).
- In CC4CL this method is not adopted for computational efficiency but could be in future versions.

As the quantity of retrieved parameters in the retrieval has increased to optimise the retrieval quality it is advisable to adopt the following *a priori* information is advised based on simulations and experience applied to real retrievals.

- An *a priori* error of 0.5 km is assumed on the upper layer CTH.
- The *a priori* lower layer CTH is assumed to be 2 ± 2 km.
- The *a priori* upper and lower layer effective radii are assumed to be 10 ± 5 and 60 ± 20 μm respectively.
- The *a priori* COT of the upper and lower layers are -1 ± 1000 (as in the standard case, note that the COT is retrieved in log as log cloud optical depth is more linear in retrieval space).
- The *a priori* surface temperature (over sea) is taken from ECMWF, with an assumed error of 1K.
- The *a priori* surface temperature (over land) is taken from ECMWF, with an assumed error of 5K.

3 Input and output data

The primary input data used by CC4CL are calibrated, geolocated satellite radiances, generally referred to as level 1 data.

- NASA M*D021KM radiance and M*D03 geolocation files are the primary input for MODIS retrievals, where the "*" represents either an "O" for MODIS-TERRA or "Y" for MODIS-AQUA data.

The physical quantity measured by satellite radiometers is radiance. Two modifications are made to the radiance for use with CC4CL: the shortwave channels are scaled by the cosine of the solar zenith angle and normalised, to produce a sun-normalised reflectance, and the thermal channel radiances are converted to brightness temperatures in Kelvin.

These files then provide CC4CL with:

- Calibrated TOA reflectance/brightness temperature;



- Solar and satellite azimuth and zenith angles;
- A land/sea mask for the level 1 grid.

CC4CL also makes use of a range of ancillary data:

- ECMWF ERA Interim humidity and temperature profiles, total column ozone, surface temperature and pressure, and 10 m east-west and north-south (u and v) wind components. These are used by the sea surface reflectance model to determine surface roughness and whitecap coverage and to estimate the sea surface emissivity.
- MODIS MCD43C1 surface BRDF product produced every 8 days with a 16-day acquisition from both Aqua and Terra-based MODIS observations [Lucht et al., 2000, Schaaf et al., 2002].
- The emissivity over land is taken from the CIMSS database [Seemann et al., 2007].
- ECMWF or SSMI snow and ice clouds masks [Nolin et al., 1998] are used to modify the surface albedo over the pole using the standard parametrisations in [Brandt et al., 2005] and [Grenfell, T. C., and D. K. Perovich, 1984]⁵.

The parameters retrieved by CC4CL are constrained to the following ranges:

- The \log_{10} of cloud optical depth at $0.55 \mu\text{m}$: [-3 – 2.408]
- The effective radius (in μm): [0.1 – 35 (liquid) or 100 (ice)]
- The cloud top pressure (in hPa): [10 – 1200]
- Surface temperature (in K): [250 – 320]

More technical descriptions of CC4CL's inputs, outputs, and data formats, in addition to example data files, can be found at the project's code repository at <http://proj.badc.rl.ac.uk/orac>.

⁵ECMWF or SSMI ice masks are used to ensure continuity in snow and ice identification for the CC4CL period. A more accurate ice/snow mask could be obtained using the 1km MODIS products



References

- Baran, A. J. and Havemann, S., The dependence of retrieved cirrus ice-crystal effective dimension on assumed ice-crystal geometry and size-distribution function at solar wavelengths, *Q. J. R. Meteorol. Soc.*, 130, 2153–2167, doi: 10.1256/qj.03.154, 2004.
- Baran A. J., Shcherbakov V.N., Baker B. A., Gayet J. F. and Lawson RP., On the scattering phase function of non-symmetric ice crystals, *Q. J. R. Meteor Soc.*, 131, 260916, 2005.
- Birks, A., Improvements to the AATSR IPF relating to land surface temperature, ESA Technical note. AATSR Product Handbook, Issue 1.2, European Space Agency, 2004.
- Brandt et al., Surface Albedo of the Antarctic Sea Ice Zone, *JOURNAL OF CLIMATE*, VOLUME 18, p3606, 2005.
- Cox, C. and Munk, W., Measurement of the roughness of the sea surface from photographs on the Sun's glitter, *J. Opt. Soc. Am.*, 44, 838–850, doi:10.1364/JOSA.44.000838, 1954.
- Cox, C. and Munk, W., Statistics of the sea surface derived from Sun glitter, *J. Mar. Res.*, 13, 198–227, 1954.
- Dee, D. P., Uppala, S. M., Simmons, A. J., Berrisford, P., Poli, P., Kobayashi, S., Andrae, U., Balmaseda, M. A., Balsamo, G., Bauer, P., Bechtold, P., Beljaars, A. C. M., van de Berg, L., Bidlot, J., Bormann, N., Delsol, C., Dragani, R., Fuentes, M., Geer, A. J., Haimberger, L., Healy, S. B., Hersbach, H., Hlm, E. V., Isaksen, L., Kllberg, P., Khler, M., Matricardi, M., McNally, A. P., Monge-Sanz, B. M., Morcrette, J.-J., Park, B.-K., Peubey, C., de Rosnay, P., Tavolato, C., Thpaut, J.-N. and Vitart, F., The ERA-Interim reanalysis: configuration and performance of the data assimilation system, *Q.J.R. Meteorol. Soc.*, 137, 553–597, doi:10.1002/qj.828, 2011.
- Grenfell, T. C., and D. K. Perovich (1984) Spectral albedos of sea ice and incident solar irradiance in the southern Beaufort Sea, *J. Geophys. Res.*, 89(C3), 3573–3580, doi:10.1029/JC089iC03p03573
- Han, Q., Rossow, W. B. and Lasis, A. A., Near-Global Survey of Effective Droplet Radii in Liquid Water Clouds Using ISCCP Data, *J. of Climate*, 7, 465–497, 1994.
- A.K. Heidinger and M. J. Pavolonis: Global daytime distribution of overlapping cirrus cloud from NOAA's Advanced Very High Resolution Radiometer. *J. Climate*, 18, 4772–4784, 2005.
- Koepke, P., Effective Reflectance of Oceanic Whitecaps, *AO*, 23, 1816–1824, doi:10.1364/AO.23.001816, 1984.
- Lean, K., Empirical methods for detecting atmospheric aerosol events from satellite measurements, MPhys. Project Report, University of Oxford, http://www.atm.ox.ac.uk/group/eodg/mphys_reports/2009_Lean.pdf, 2009.
- Levenberg, K., A method for the solution of certain nonlinear problems in least squares, *Quart. Appl. Math.*, 2, 164–168, 1944.
- Lucht, W., Schaaf, C.B., and Strahler, A.H., An Algorithm for the Retrieval of Albedo from Space Using Semiempirical BRDF Models, *Atmospheric Science, Surface Radiative Properties/BRDFs, TGRS*, 38, 977–998, doi:10.1109/36.841980, 2000.
- Nolin, A., Armstrong, R. L. and Maslanik, J., Near-Real-Time SSM/I-SSMIS EASE-Grid Daily Global Ice Concentration and Snow Extent. Boulder, Colorado USA: National Snow and Ice Data Center, 1998.



- Marquardt, D. W., An algorithm for least-squares estimation of nonlinear parameters, *SIAM, J. Appl. Math.*, 11, 431–441, doi:10.2307/2098941, 1963.
- Morel, A. and Prieur, L., Analysis of Variations in Ocean Color, *Limnology and Oceanography*, 22, 709–722, doi:10.4319/lo.1977.22.4.0709, 1977.
- Mcgarraugh, G. CC4CL Cloud retrievals paper in preparation.
- MTG Level 2 Processing Specification Document, Document Number EUM/MTG/SPE/12/1078, March 2014.
- Pavolonis, M. J. and Heidinger A. K., Daytime Cloud Overlap Detection from AVHRR and VIIRS, *J. Appl. Meteor.*, 43, 762–778, doi:10.1175/2099.1, 2004.
- Pavolonis, M. J., Heidinger A. K., and Uttal, T., Daytime Global Cloud Typing from AVHRR and VIIRS: Algorithm Description, Validation, and Comparisons, *J. Appl. Meteor.*, 44, 804–826, doi:10.1175/JAM2236.1, 2005.
- Poulsen, C. A., Siddans, R., Thomas, G. E., Sayer, A. M., Grainger, R. G., Campmany, E., Dean, S. M., Arnold, C., and Watts, P. D., Cloud retrievals from satellite data using optimal estimation: evaluation and application to ATSR, *Atmos. Meas. Tech.*, 5, 1889–1910, doi:10.5194/amt-5-1889-2012, 2012.
- Rodgers, C. D., Inverse methods for atmospheric sounding: Theory and Practice. Series on Atmospheric, Oceanic and Planetary Physics, Vol. 2, World Scientific, 2000.
- Saunders, R. W., Matricardi, M. and Brunel, P., An Improved Fast Radiative Transfer Model for Assimilation of Satellite Radiance Observations, *Q. J. R. Meteor. Soc.*, 125, 1407–1425, 1999.
- Sayer A. M, Poulsen, C. A., Arnold, C., Campmany, E., Dean, S., Ewen, G. B. L., Grainger, R. G., Lawrence, B. N., Siddans, R., Thomas, G. E., and Watts, P. D., Global retrieval of ATSR cloud parameters and evaluation (GRAPE): dataset assessment *Atmos. Chem. Phys.*, 11, 3913–3936, doi:10.5194/acp-11-3913-2011, 2011.
- Sayer, A. M., Thomas, G. E. and Grainger, R. G., A sea surface reflectance model for (A)ATSR, and application to aerosol retrievals, *Atmos. Meas. Tech.*, 2010, 3, 813–838, 4, 2010
- Schaaf, C. B., F. Gao, A. H. Strahler, W. Lucht, X. Li, T. Tsang, N. C. Strugnell, X. Zhang, Y. Jin, J.-P. Muller, P. Lewis, M. Barnsley, P. Hobson, M. Disney, G. Roberts, M. Dunderdale, C. Doll, R. d’Entremont, B. Hu, S. Liang, and J. L. Privette, and D. P. Roy., First Operational BRDF, Albedo and Nadir Reflectance Products from MODIS, *Remote Sens. Environ.*, 83, 135–148, 2002.
- Schaepman-Strub, G., Schaepman, M. E., Painter, T. H., Dangel, S., Martonchik J. V., Reflectance quantities in optical remote sensing — definitions and case studies., *Remote Sens. Environ.*, 103, 27–42, 2006.
- Seemann, S. W., Borbas, E. E., Knuteson, R. O., Stephenson, G. R. and Huang, H.-L. Development of a Global Infrared Land Surface Emissivity Database for Application to Clear Sky Sounding Retrievals from Multi-spectral Satellite Radiance Measurements., *Appl. Meteor. Climatol.*, 47, 108–123, 2007.
- R. Siddans, C. Poulsen, E. Carboni Cloud Model for Operational Retrievals from MSG SEVIRI Final Report DRAFT Version 1.0, Eumetsat Contract EUM/CO/07/4600000463/PDW, January 26, 2011
- Stamnes K., Tsay S.C., Wiscombe W. and Jayaweera K., Numerically stable algorithm for discrete ordinate method radiative transfer in multiple scattering and emitting layered media., *Appl. Opt.*, 12, 2502–2509, 1988.



- Takano, Y., and Liou, K. N., Solar radiative transfer in cirrus clouds. Part I: Single-scattering and optical properties of hexagonal ice crystals., *J. Atmos. Sci.*, 46, 3–19, 1989.
- Thomas, G. E., Carboni, E., Sayer, A. M., Poulsen, C. A., Siddans, R. and Grainger, R. G., Oxford-RAL Aerosol and Cloud (ORAC): aerosol retrievals from satellite radiometers, in *Satellite aerosol remote sensing over land*, Kokhanovsky, A. A. and de Leeuw, G. (eds.), Springer-Praxis, 2009.
- Wanner, W., Strahler, A. H., Hu, B., Lewis, P., Muller, J.-P., Li, X., Barker Schaaf, C. L., and Barnsley, M. J., Global Retrieval of Bidirectional Reflectance and Albedo Over Land from EOS MODIS and MISR Data: Theory and Algorithm, *JGR*, 102, D14, 17143–17161, doi:10.1029/96JD03295, 1997.
- Watts, P. D., Mutlow, C. T., Baran, A. J. and Zavody, A. M., Study on cloud properties derived from Meteosat Second Generation Observations. Eumetsat Report, <http://www.eumetsat.int/Home/index.htm>, 1998
- P.D. Watts, R. Bennatz and F. Fell: Retrieval of two-layer cloud properties from multispectral observations using optimal estimation. *J. Geophys. Res.*, 116, D16203, doi:10.1029/2011JD015883, 2011.
- Zhang Z., Yang, P., Kattawar, G., Riedi, J., Labonnote, L. C.-, Baum, B. A., Platnick, S., and Huang, H.-L., Influence of ice particle model on satellite ice cloud retrieval: lessons learned from MODIS and POLDER cloud product comparison, *Atmos. Chem. Phys.*, 9, 7115–7129, 2009.